

Supporting Information : Effect of stepwise protonation of an N-containing ligand on the formation of metal-organic salts and coordination complexes in the solid state

Haidong Lv [‡], Haitao Li [‡], Lianxin Xin, and Fang Guo*

[‡] These authors made equal contributions to this work.

College of Chemistry, Liaoning University, Shenyang, 110036, China.

Contents

Figure S1. The experimental powders of protonated ligands by grinding L and HX (X=Cl, Br, I).

Figure S2. Comparison of experimental and simulated PXRD patterns for crystal $[2\text{HL}]^{2+}\cdot 2\text{Cl}^-$.

Figure S3. Comparison of experimental and simulated PXRD patterns for crystal $[4\text{HL}]^{4+}\cdot 4\text{Cl}^-$.

Figure S4. Comparison of experimental and simulated PXRD patterns for crystal $[4\text{HL}]^{4+}\cdot 4\text{I}^-\cdot 2\text{CH}_3\text{OH}$.

Figure S5. Comparison of experimental and simulated PXRD patterns for crystal **1**.

Figure S6. Comparison of experimental and simulated PXRD patterns for crystal **1'**.

Figure S7. Comparison of experimental and simulated PXRD patterns for crystal **2**.

Figure S8. Comparison of experimental and simulated PXRD patterns for crystal **2'**.

Figure S9. Comparison of experimental and simulated PXRD patterns for crystal **3**.

Figure S10. Comparison of experimental and simulated PXRD patterns for crystal **3'**.

Figure S11. Comparison of experimental and simulated PXRD patterns for crystal **4**.

Figure S12. Comparison of experimental and simulated PXRD patterns for crystal **4'**.

Figure S13. Images of the crystals **1-4'**.

Figure S14. Reversible adsorption experiment of crystal **1** and **1'**.

Figure S15. *Ex situ* PXRD patterns of salt **1'** absorbing HCl after four weeks.

Figure S16. The experimental powders of grinding different protonation ligands ($[2\text{HL}]^{2+}\cdot 2\text{X}^-$, $[4\text{HL}]^{4+}\cdot 4\text{X}^-$ (X=Cl, Br, I)) and ZnX_2 (X=Cl, Br, I).

Figure S17. TG curve of crystals **1** and **1'**.

Figure S18. TG curve of crystals **2** and **2'**.

Figure S19. TG curve of crystals **3** and **3'**.

Figure S20. TG curve of crystal **4** and **4'** (the poor stability of crystals led to the inaccurate results of TGA).

Figure S21. Crystal structure of **4** (a) and **4'** (b) showing the charge assisted hydrogen bonding interactions among $[2\text{HL}]^{2+}$ and $[\text{N}_{\text{pyridine}}\text{-ZnBr}_3]^-$ (dashed lines) with methanol or water involved in it.

Figure S22. PXRD of (a) simulated PXRD of **4** from SC-XRD data, and (b) The products of exposing **4** to the air shortly after it was taken out from the mother solution.

Figure S23. PXRD of (a) simulated PXRD of **4'** from SC-XRD data, and (b) The products of exposing **4'** to the air shortly after it was taken out from the mother solution.

Table S1. Crystallographic data for crystals $[4\text{HL}]^{4+}\cdot 4\text{I}^- \cdot 2\text{CH}_3\text{OH}$ and **1-4'**.

Table S2. Hydrogen bonding data of crystal **1**.

Table S3. Hydrogen bonding data of crystal **1'**.

Table S4. Hydrogen bonding data of crystal **2**.

Table S5. Hydrogen bonding data of crystal **2'**.

Table S6. Hydrogen bonding data of crystal **3**.

Table S7. Hydrogen bonding data of crystal **3'**.

Table S8. Hydrogen bonding data of crystal **4**.

Table S9. Hydrogen bonding data of crystal **4'**.

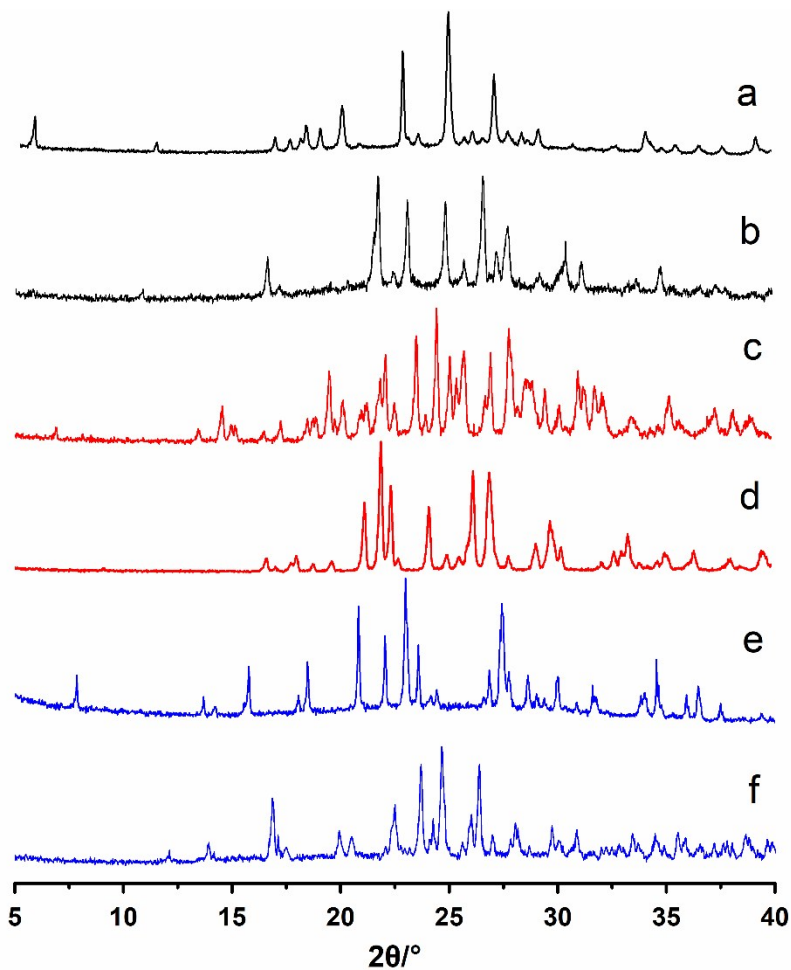


Figure S1. The experimental powders of protonated ligands by grinding L and HX ($X=Cl, Br, I$): (a) $[2HL]^{2+}\cdot 2Cl^-$; (b) $[4HL]^{4+}\cdot 4Cl^-$; (c) $[2HL]^{2+}\cdot 2Br^-$; (d) $[4HL]^{4+}\cdot 4Br^-$; (e) $[2HL]^{2+}\cdot 2I^-$; (f) $[4HL]^{4+}\cdot 4I^-\cdot 2CH_3OH$.

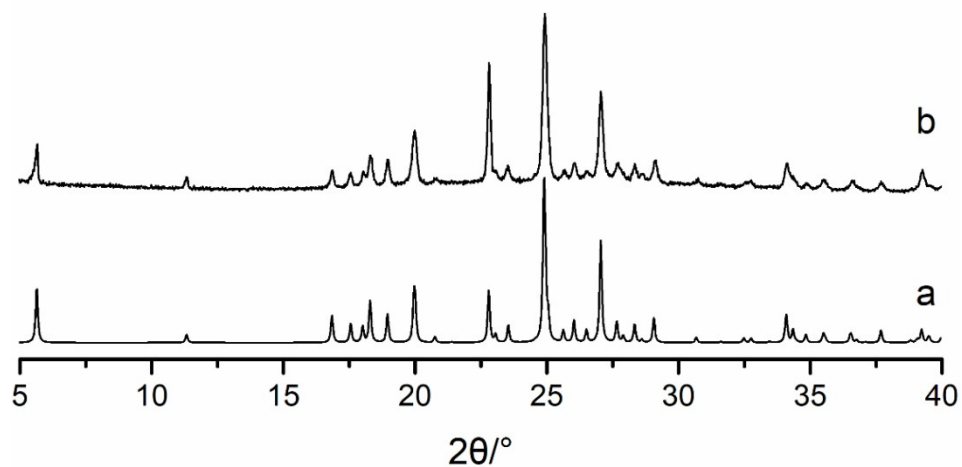


Figure S2. (a) Simulated PXRD of reported single crystal data of $[2HL]^{2+}\cdot 2Cl^-$. (b) Experimental PXRD from single crystal $[2HL]^{2+}\cdot 2Cl^-$.

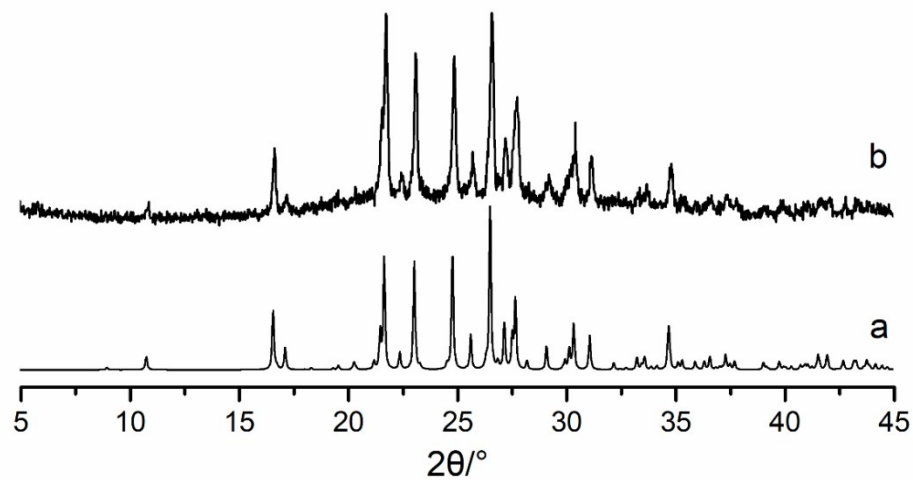


Figure S3. (a) Simulated PXRD of reported single crystal data of $[4\text{HL}]^{4+} \cdot 4\text{Cl}^-$. (b) Experimental PXRD from single crystal $[4\text{HL}]^{4+} \cdot 4\text{Cl}^-$.

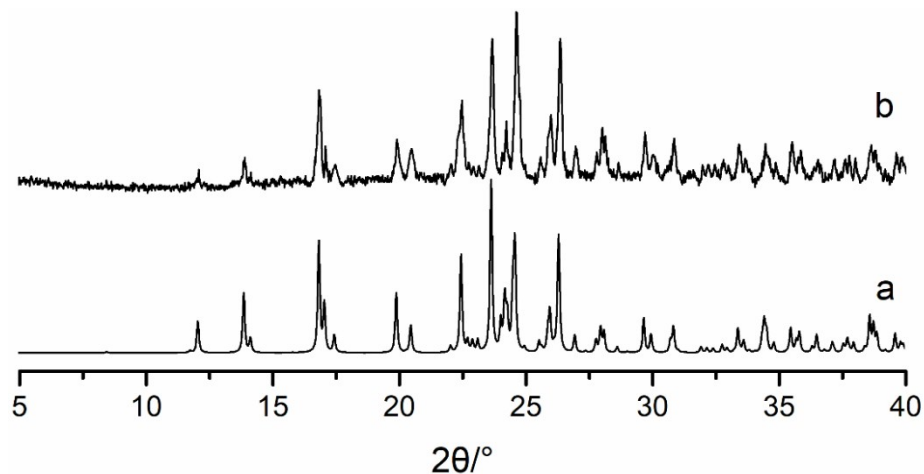


Figure S4. (a) Simulated PXRD of reported single crystal data of $[4\text{HL}]^{4+} \cdot 4\text{I}^- \cdot 2\text{CH}_3\text{OH}$. (b) Experimental PXRD from single crystal $[4\text{HL}]^{4+} \cdot 4\text{I}^- \cdot 2\text{CH}_3\text{OH}$.

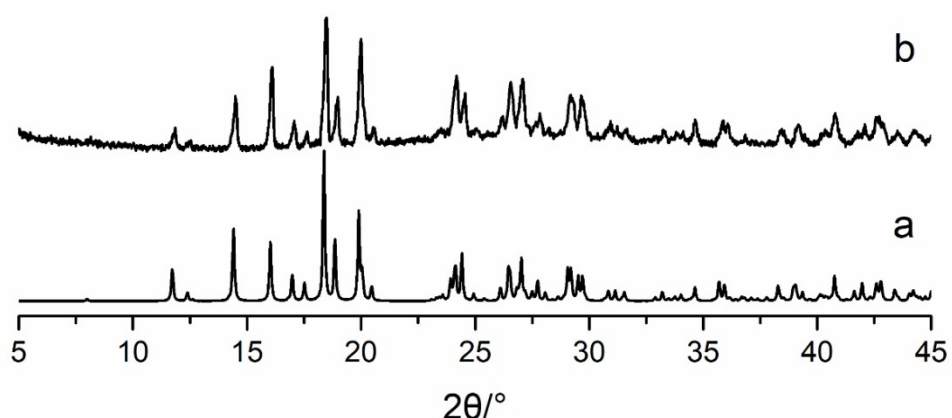


Figure S5. (a) Simulated PXRD of **1** from SC-XRD data. (b) Experimental PXRD from single crystal **1**.

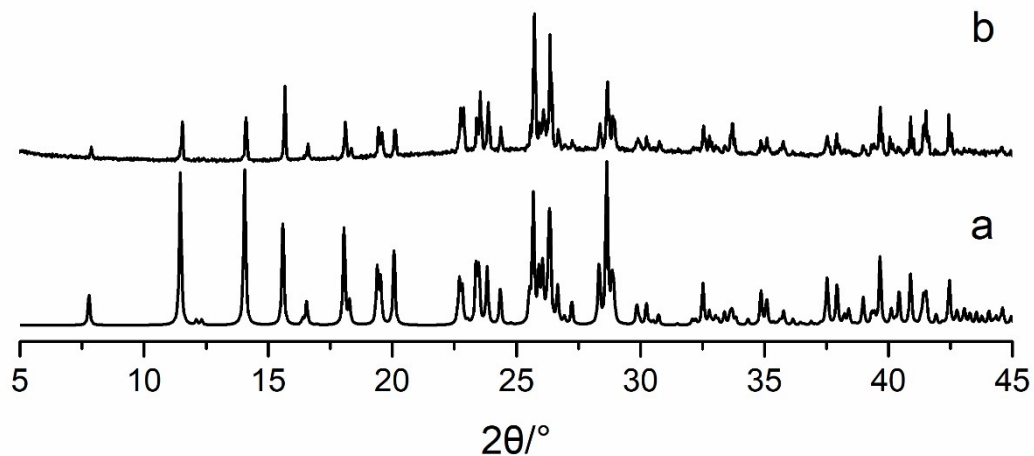


Figure S6. (a) Simulated PXRD of **1'** from SC-XRD data. (b) Experimental PXRD from single crystal **1'**.

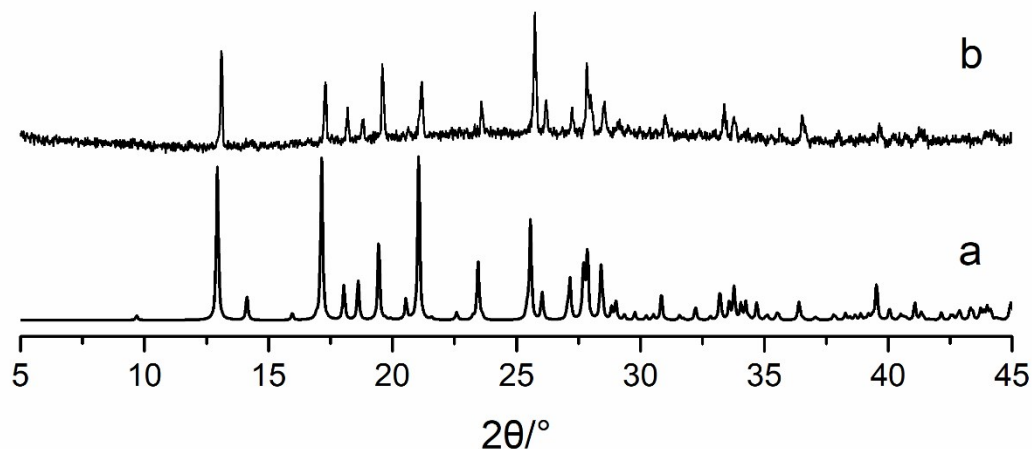


Figure S7. (a) Simulated PXRD of **2** from SC-XRD data. (b) Experimental PXRD from single crystal **2**.

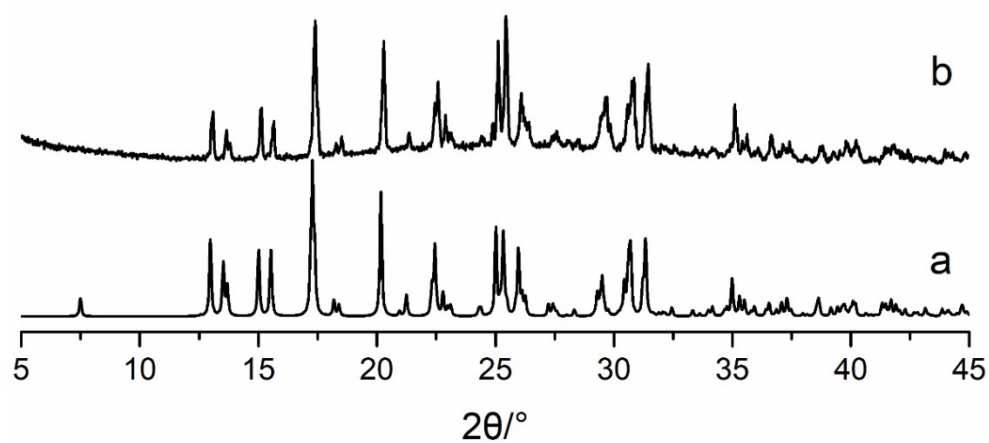


Figure S8. (a) Simulated PXRD of **2'** from SC-XRD data. (b) Experimental PXRD from single crystal **2'**.

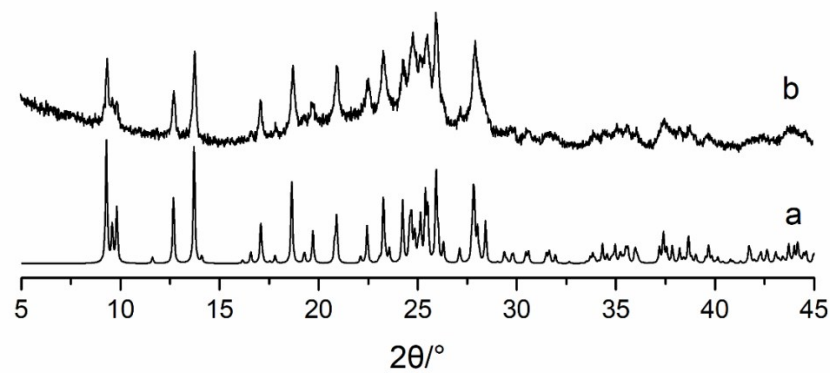


Figure S9. (a) Simulated PXRD of **3** from SC-XRD data. (b) Experimental PXRD from single crystal **3**.

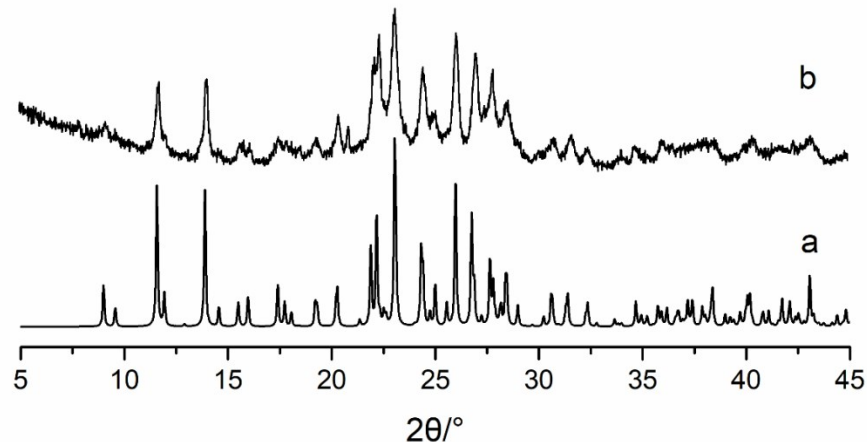


Figure S10. (a) Simulated PXRD of **3'** from SC-XRD data. (b) Experimental PXRD from single crystal **3'**.

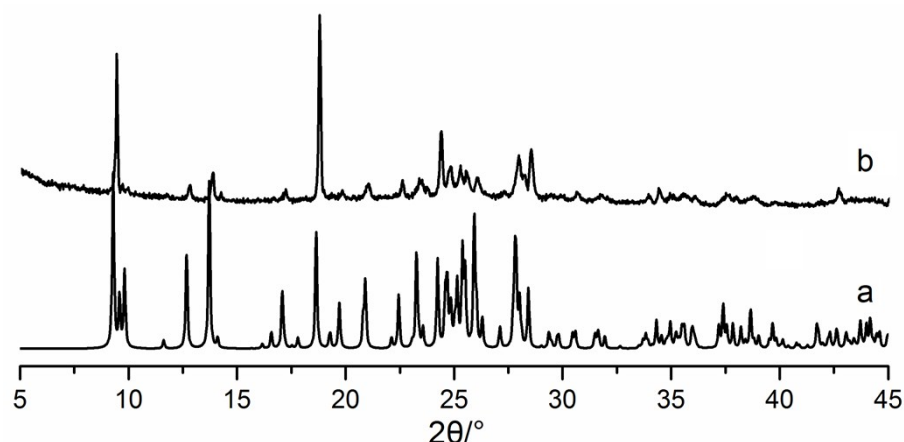


Figure S11. (a) Simulated PXRD of **4** from SC-XRD data. (b) Experimental PXRD from single crystal **4**.

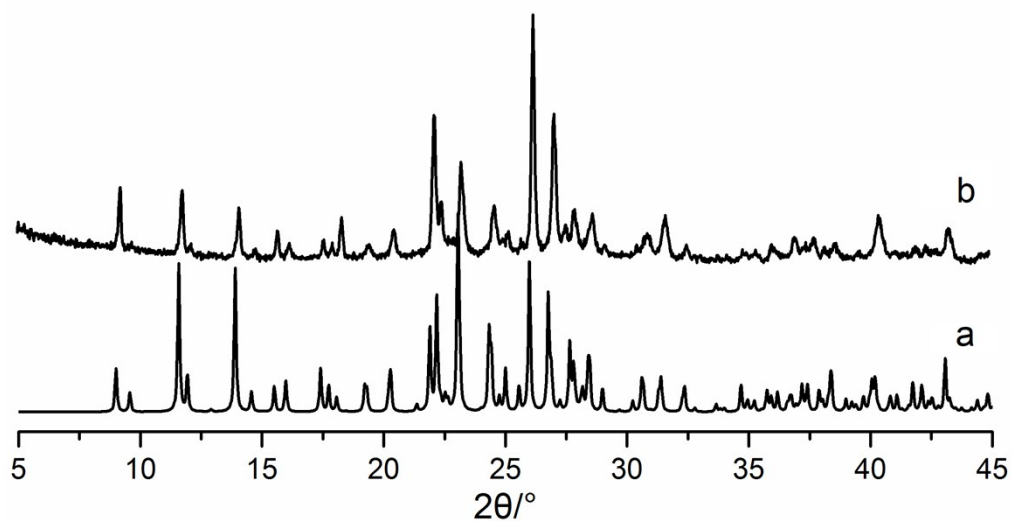


Figure S12. (a) Simulated PXRD of **4'** from SC-XRD data. (b) Experimental PXRD from single crystal **4'**.

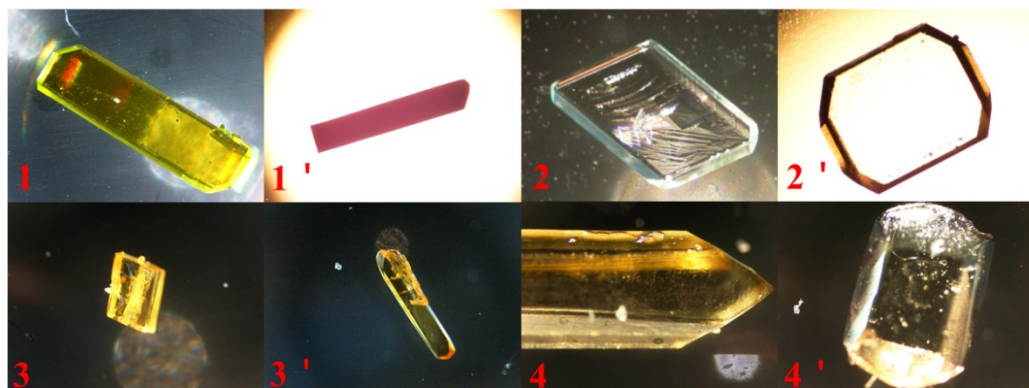


Figure S13. Images of the crystals **1-4'**.

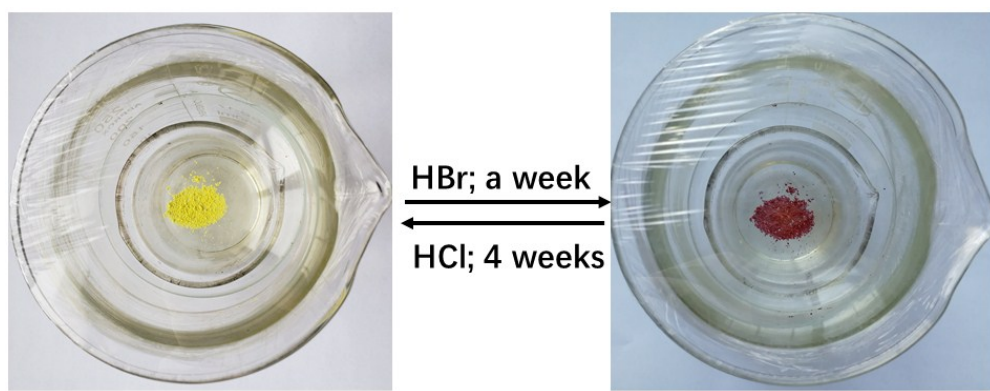


Figure S14. Reversible adsorption experiment of crystal **1** and **1'**.

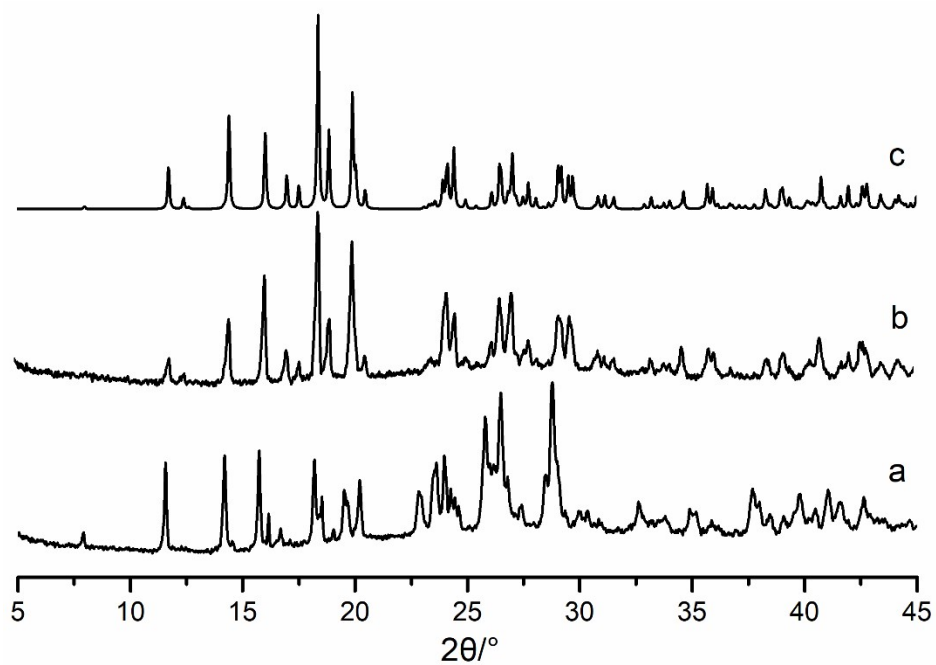


Figure S15. (a) Experimental PXRD from single crystal **1'**. (b) PXRD patterns of salt **1'** absorbing HCl after four weeks. (c) Experimental PXRD from single crystal **1**.

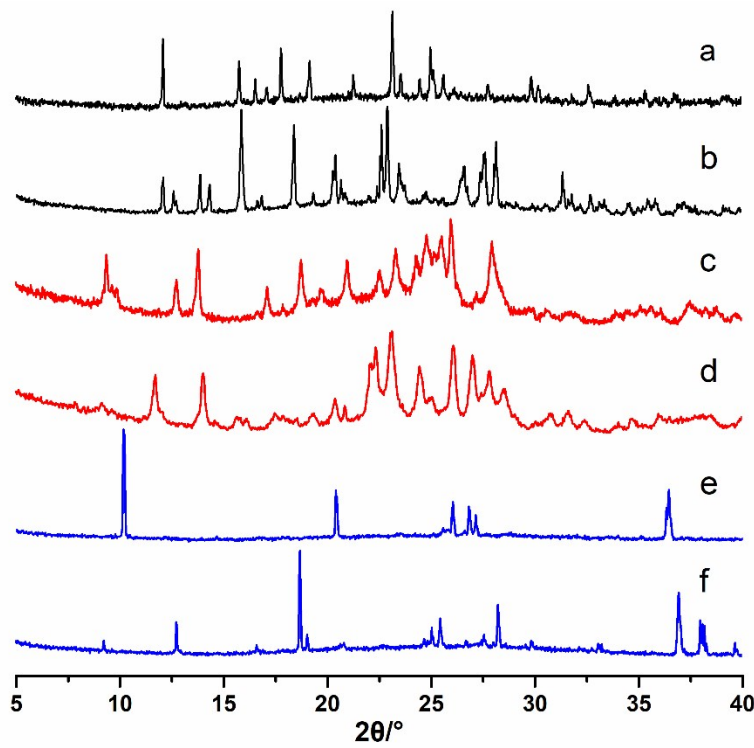


Figure S16. The experimental powders of grinding different protonation ligands ($[2\text{HL}]^{2+} \cdot 2\text{X}^-$, $[4\text{HL}]^{4+} \cdot 4\text{X}^-$ ($\text{X} = \text{Cl}, \text{Br}, \text{I}$)) and ZnX_2 ($\text{X} = \text{Cl}, \text{Br}, \text{I}$): (a) **2**; (b) **2'**; (c) **3**; (d) **3'**; (e) the product of grinding $[2\text{HL}]^{2+} \cdot 2\text{Br}^-$ with ZnBr_2 in a 1:2 molar ratio; (f) the product of grinding $[4\text{HL}]^{4+} \cdot 2\text{Br}^-$ with ZnBr_2 in a 1:2 molar ratio.

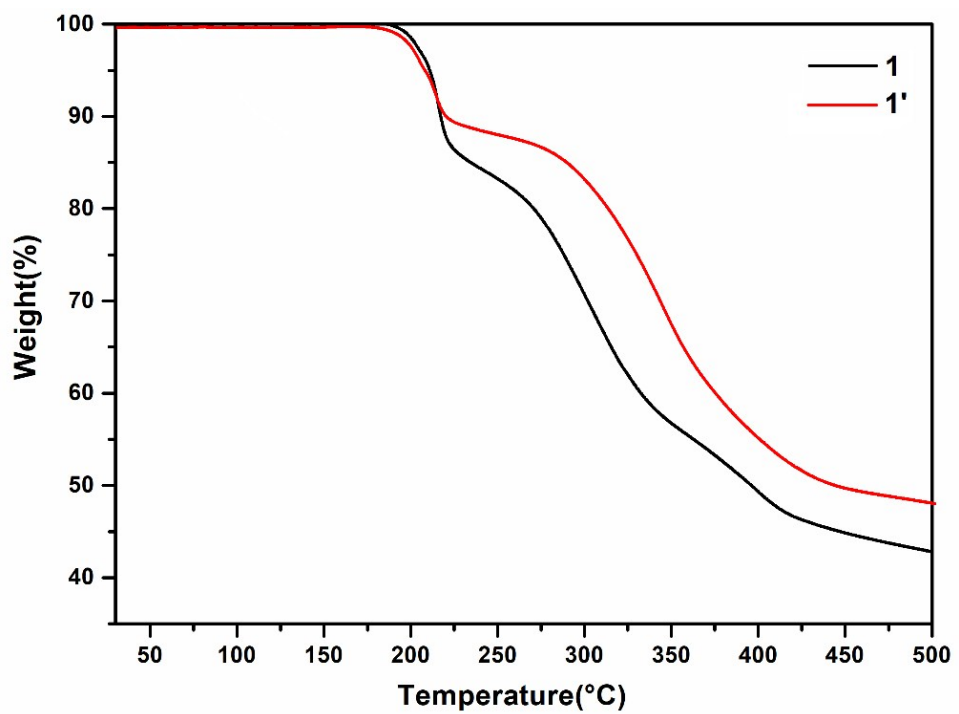


Figure S17. TG curve of crystal 1 and 1'.

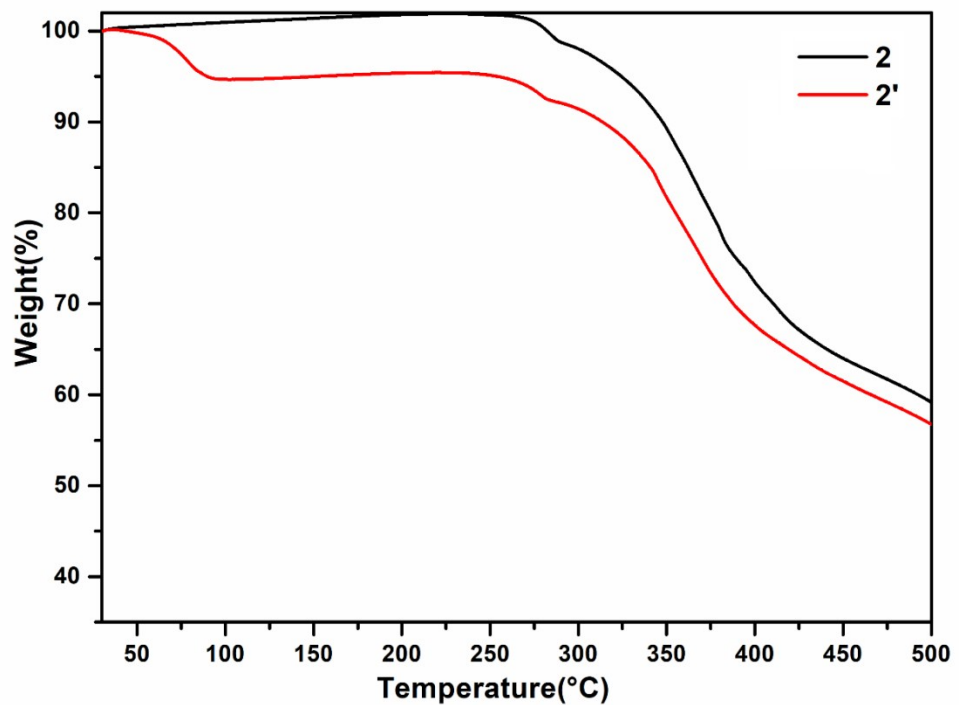


Figure S18. TG curve of crystal 2 and 2'.

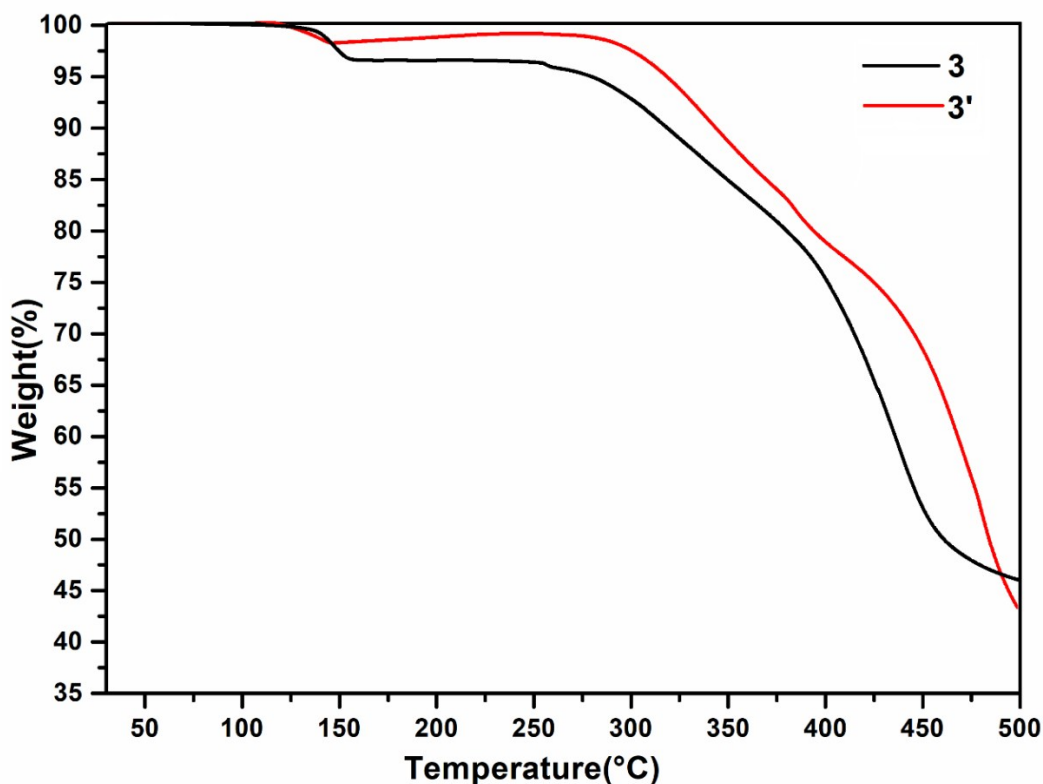


Figure S19. TG curve of crystal 3 and 3'.

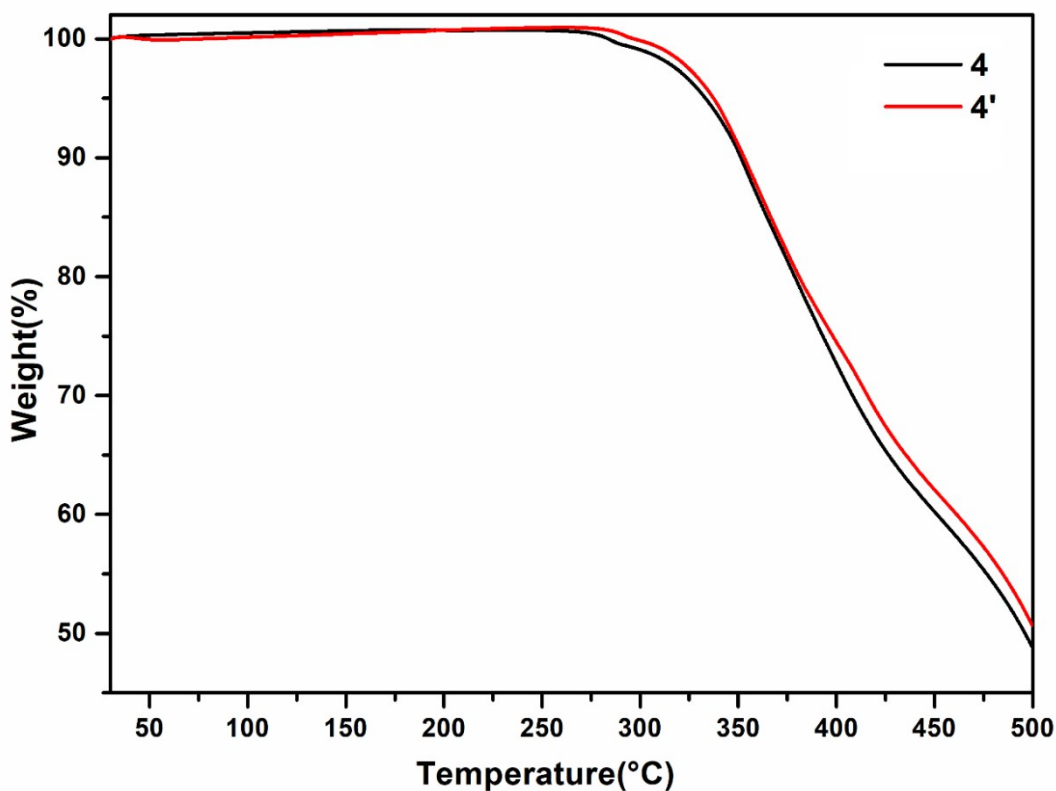


Figure S20. TG curve of crystal 4 and 4' (the poor stability of crystals led to the inaccurate results of TGA).

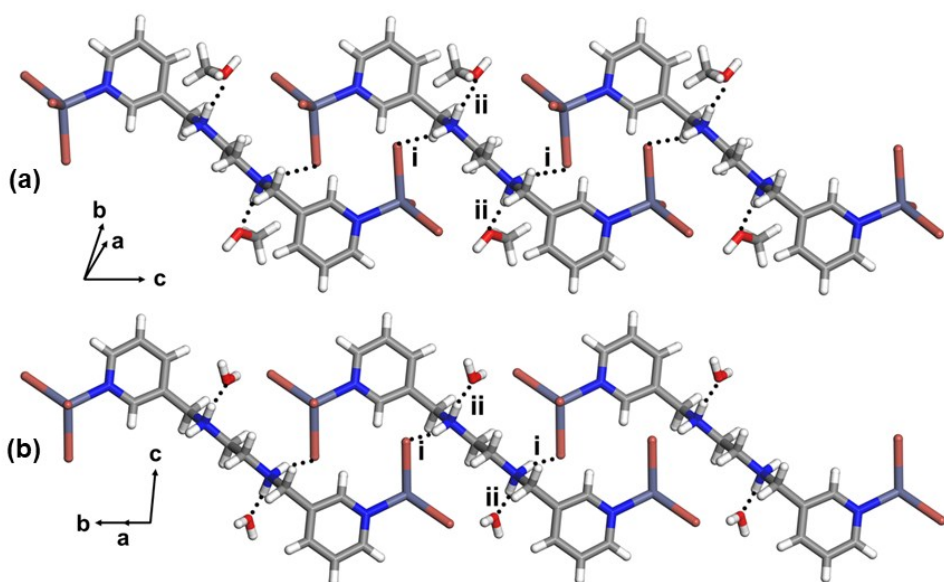


Figure S21. Crystal structure of **4** (a) and **4'** (b) showing the charge assisted hydrogen bonding interactions among $[2\text{HL}]^{2+}$ and $[\text{N}_{\text{pyridine}}\text{-ZnBr}_3]^-$ (dashed lines) with methanol or water involved in it.

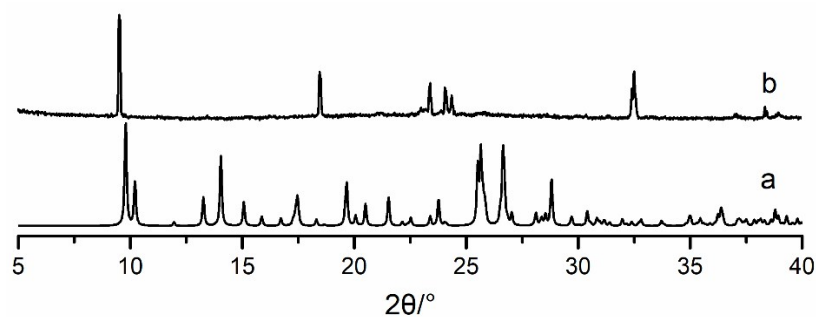


Figure S22. PXRD of (a) simulated PXRD of **4** from SC-XRD data, and (b) The products of exposing **4** to the air shortly after it was taken out from the mother solution.

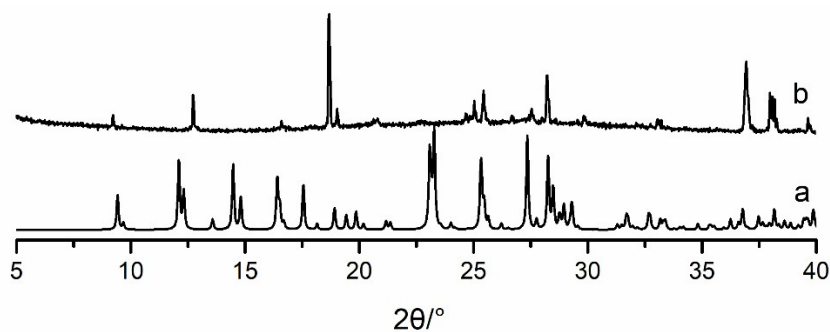


Figure S23. PXRD of (a) simulated PXRD of **4'** from SC-XRD data, and (b) The products of exposing **4'** to the air shortly after it was taken out from the mother solution.

Table S1. Crystallographic data for crystals $[4\text{HL}]^{4+}\cdot 4\text{I}^- \cdot 2\text{CH}_3\text{OH}$ and **1-4'**.
Crystallographic data for crystals **2** and **2'**.

	$[4\text{HL}]^{4+}\cdot 4\text{I}^- \cdot 2\text{CH}_3\text{OH}$	1	1'
Empirical formula	$\text{C}_{16}\text{H}_{30}\text{I}_4\text{N}_4\text{O}_2$	$\text{C}_{14}\text{H}_{22}\text{Cl}_8\text{Cu}_2\text{N}_4$	$\text{C}_{14}\text{H}_{22}\text{Br}_8\text{Cu}_2\text{N}_4$
Formula weight	818.04	657.03	1012.17
Crystal temperature (K)	293	298	293
Crystal system	Monoclinic	Monoclinic	Monoclinic
Space group	$P2_1/c$	$P2_1/c$	$P2_1/c$
Z	2	2	2
a(Å)	8.0705(6)	7.552 (3)	7.7157(13)
b(Å)	20.8072(16)	22.128 (8)	22.709(4)
c(Å)	7.8346(6)	7.398 (3)	7.5681(13)
α (deg)	90	90	90
β (deg)	93.907(3)	91.831 (11)	90.842(7)
γ (deg)	90	90	90
V(Å ³)	1312.56(17)	1235.7(8)	1325.9(4)
Dx(Mg.cm ⁻³)	2.070	1.766	2.537
μ (mm ⁻¹)	4.764	2.596	13.668
F(000)	0.0545	656.0	944.0
No. of data with $I > 2\sigma(I)$	0.029	0.0554	0.0598
No. of parameter	16112	13657	20406
R _{int}	2201	2668	3321
s	120	127	131
No. of collected data(unique)	1.200	1.231	1.197
$[I \geq 2\sigma(I)]R_1/wR_2$	0.0409/0.0943	0.0669/0.1644	0.0662/0.1533
All data R ₁ /wR ₂	0.0416/0.0947	0.0714/0.1673	1012.17

Crystallographic data for crystals **2** and **2'**.

	2	2'
Empirical formula	$\text{C}_{14}\text{H}_{22}\text{Cl}_8\text{N}_4\text{Zn}_2$	$\text{C}_{14}\text{H}_{26}\text{Cl}_8\text{N}_4\text{O}_2\text{Zn}_2$
Formula weight	660.69	696.73
Crystal temperature (K)	298	295.07
Crystal system	Monoclinic	Monoclinic
Space group	$P2_1/n$	$P2_1/c$
Z	2	2

a(Å)	10.2666(6)	12.2223(6)
b(Å)	9.5232(6)	8.3549(4)
c(Å)	13.0868(8)	13.5644 (7)
α (deg)	90	90
β (deg)	106.857(2)	105.261 (2)
γ (deg)	90	90
V(Å ³)	1224.53(13)	1336.30 (12)
Dx(Mg.cm ⁻³)	1.792	1.818
μ (mm ⁻¹)	2.841	2.807
F(000)	660.0	728.0
No. of data with I>2σ (I)	2993	3294
No. of parameter	127	136
R _{int}	0.0223	0.0417
s	1.121	1.065
No. of collected data(unique)	20162	19659
[I>=2σ (I)]R ₁ /wR ₂	0.0268/0.0647	0.0521/0.1508
All data R ₁ /wR ₂	0.0287/0.0662	0.0558/0.1548

Crystallographic data for crystals **3** and **3'**.

	3	3'
Empirical formula	C ₁₆ H ₂₈ I ₆ N ₄ O ₂ Zn ₂	C ₁₄ H ₂₄ I ₆ N ₄ O ₂ Zn ₂
Formula weight	1200.56	1172.51
Crystal temperature (K)	296	296
Crystal system	Triclinic	Triclinic
Space group	P-1	P-1
Z	1	1
a(Å)	7.9785 (5)	7.7826 (18)
b(Å)	10.7150 (7)	9.850 (2)
c(Å)	10.8206 (7)	10.106 (2)
α (deg)	63.205 (2)	101.146(6)
β (deg)	73.580 (2)	94.713 (6)
γ (deg)	87.892 (2)	105.848(6)
V(Å ³)	787.59 (9)	723. 7 (3)
Dx(Mg.cm ⁻³)	2.531	2.6

$\mu(\text{mm}^{-1})$	7.421	8.073
F(000)	546.0	530.0
No. of data with $I > 2\sigma(I)$	3767	2478
No. of parameter	145	130
R_{int}	0.0330	0.0470
s	1.182	1.131
No. of collected data(unique)	12358	13372
$[I \geq 2\sigma(I)]R_1/wR_2$	0.0360/0.0830	0.0656/0.1968
All data R_1/wR_2	0.0391/0.0859	0.0670/0.1989

Crystallographic data for crystals **4** and **4'**.

	4	4'
Empirical formula	$C_{16}H_{24}Br_6N_4O_2Zn_2$	$C_{14}H_{24}Br_6N_4O_2Zn_2$
Formula weight	918.60	890.55
Crystal temperature (K)	298	298
Crystal system	triclinic	triclinic
Space group	<i>P</i> -1	<i>P</i> -1
Z	1	1
a(Å)	7.7044 (9)	7.458 (5)
b(Å)	10.1649 (13)	9.586(6)
c(Å)	10.5702 (13)	9.603 (6)
α (deg)	62.697 (4)	99.830 (18)
β (deg)	74.100 (5)	95.106 (18)
γ (deg)	85.369 (5)	103.695 (19)
$V(\text{\AA}^3)$	706.46 (15)	651.27 (7)
$D_x(\text{Mg.cm}^{-3})$	2.159	2.271
$\mu(\text{mm}^{-1})$	10.201	11.063
F(000)	438.0	422.0
No. of data with $I > 2\sigma(I)$	2119	1748
No. of parameter	139	131
R_{int}	0.0549	0.0553
s	1.190	1.197
No. of collected data(unique)	5335	3741
$[I \geq 2\sigma(I)]R_1/wR_2$	0.1129/0.2664	0.0966/0.2295
All data R_1/wR_2	0.1191/0.2697	0.1155/0.2491

Table S2. Hydrogen bonding data of crystal **1**.

Interactions(D-H···A)	D-H (Å)	H···A (Å)	D···A (Å)	D-H···A (°)
N1-H1B···Cl2(i)	0.891	2.463	3.237	145.56
N1-H1A···Cl4(ii)	0.889	2.388	3.133	141.50
N2-H2···Cl1(iii)	0.860	2.353	3.148	153.92

Table S3. Hydrogen bonding data of crystal **1'**.

Interactions(D-H···A)	D-H (Å)	H···A (Å)	D···A (Å)	D-H···A (°)
N1-H1A···Br3(i)	0.890	2.567	3.303	140.59
N1-H1B···Br4(ii)	0.890	2.629	3.387	143.54
N2-H2···Br1(iii)	0.791	2.593	3.289	147.70

Table S4. Hydrogen bonding data of crystal **2**.

Interactions(D-H···A)	D-H (Å)	H···A (Å)	D···A (Å)	D-H···A (°)
N2-H2···Cl2(i)	0.860	2.642	3.224	136.11
N1-H1B···Cl4(ii)	0.890	2.275	3.117	157.54
N1-H1A···Cl1(iii)	0.890	2.358	3.169	151.60
N2-H2···Cl1(iv)	0.860	2.562	3.265	139.65

Table S5. Hydrogen bonding data of crystal **2'**.

Interactions(D-H···A)	D-H (Å)	H···A (Å)	D···A (Å)	D-H···A (°)
N1-H1A···Cl2(i)	0.890	2.590	3.278	134.78
N1-H1B···O1(ii)	0.890	1.885	2.769	171.50
O1-H1F···Cl3(iii)	0.850	2.326	3.164	169.00
N2-H2···Cl1(iv)	0.860	2.333	3.165	162.92

Table S6. Hydrogen bonding data of crystal **3**.

Interactions(D-H···A)	D-H (Å)	H···A (Å)	D···A (Å)	D-H···A (°)
N1-HA···I1(i)	0.921	2.626	3.528	166.60
N1-HB···O(ii)	0.818	1.933	2.747	173.02
C2-H2A···I2(iii)	0.970	3.156	3.783	123.85

Table S7. Hydrogen bonding data of crystal **3'**.

Interactions(D-H···A)	D-H (Å)	H···A (Å)	D···A (Å)	D-H···A (°)
N1-HA···I1(i)	0.890	2.736	3.545	151.57
N1-HB···O(ii)	0.890	1.820	2.695	166.90
O1-H1E···I3(iii)	0.850	3.007	3.646	133.68
C6-H1F···O(iv)	0.930	2.695	3.613	168.98

Table S8. Hydrogen bonding data of crystal **4**.

Interactions(D-H···A)	D-H (Å)	H···A (Å)	D···A (Å)	D-H···A (°)
N1-HA···Br1(i)	0.888	2.432	3.307	168.36
N1-HB···O(ii)	0.892	1.837	2.721	173.33
C2-H2A···Br2(iii)	0.970	3.156	3.783	123.85

Table S9. Hydrogen bonding data of crystal **4'**.

Interactions(D-H···A)	D-H (Å)	H···A (Å)	D···A (Å)	D-H···A (°)
N1-H1A···Br3(i)	0.890	2.512	3.334	153.97
N1-H1B···O(ii)	0.890	1.816	2.691	164.15
O1-H1E···Br3(iii)	0.850	3.007	3.646	133.68
C6-H1F···O(iv)	0.930	2.695	3.613	168.98